Electronic Supplementary Material (ESI) for Energy & Environmental Science

Supporting Information: Influence of Dye Adsorption on the TiO_2 Conduction Band Energetics in Dye-Sensitized Solar Cells Models: Disentangling Charge Transfer and Electrostatic Effects.

Enrico Ronca,[a,b] Mariachiara Pastore,[a] Leonardo Belpassi,[a] Francesco Tarantelli,[a,b] Filippo De Angelis [a]*

[a] Computational Laboratory for Hybrid/Organic Photovoltaics (CLHYO), Istituto CNR di Scienze e Tecnologie Molecolari, via Elce di Sotto 8, I-06123, Perugia, Italy

[b] Dipartimento di Chimica, Università degli Studi di Perugia, via Elce di Sotto 8, I-06123, Perugia, Italy

E-mail: filippo@thch.unipg.it

Electronic Supplementary Information

Charge Displacement Curves

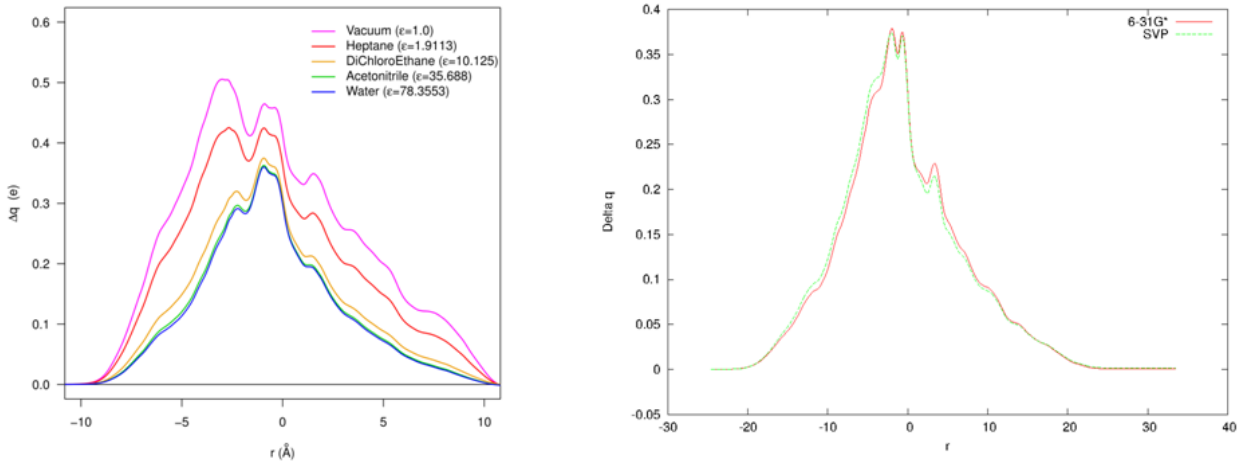

Fig. S1: Left: CD curve of the L0-TiO_2 system anchored in BB geometry as a function of different solvents. Right: comparison between the CD curves calculated by SVP and 6-31G* basis sets for the same system.

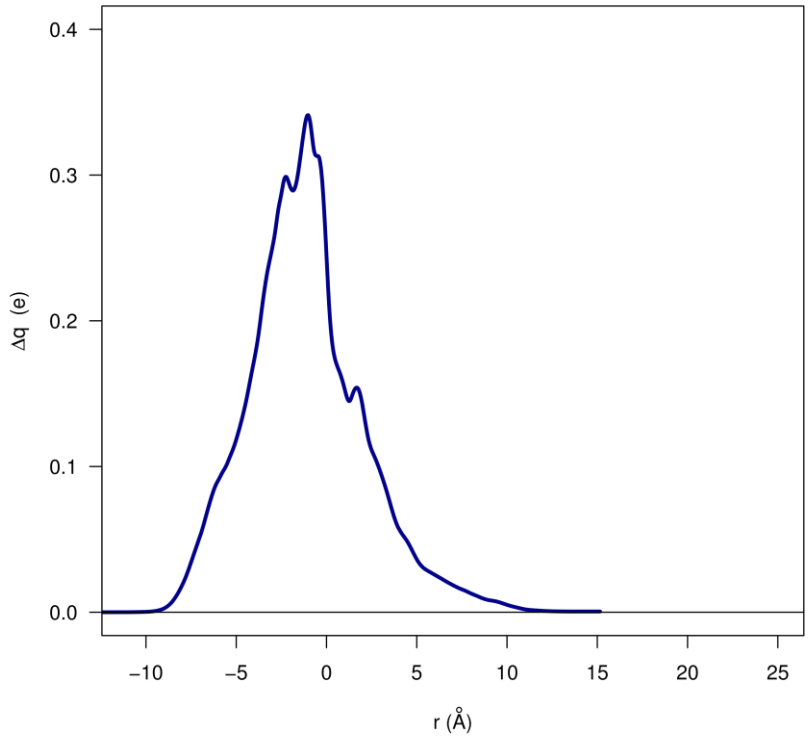

Fig. S2: CD curve of the rh-L0-TiO_2 system. The sensitizer is anchored on TiO_2 in BB geometry.

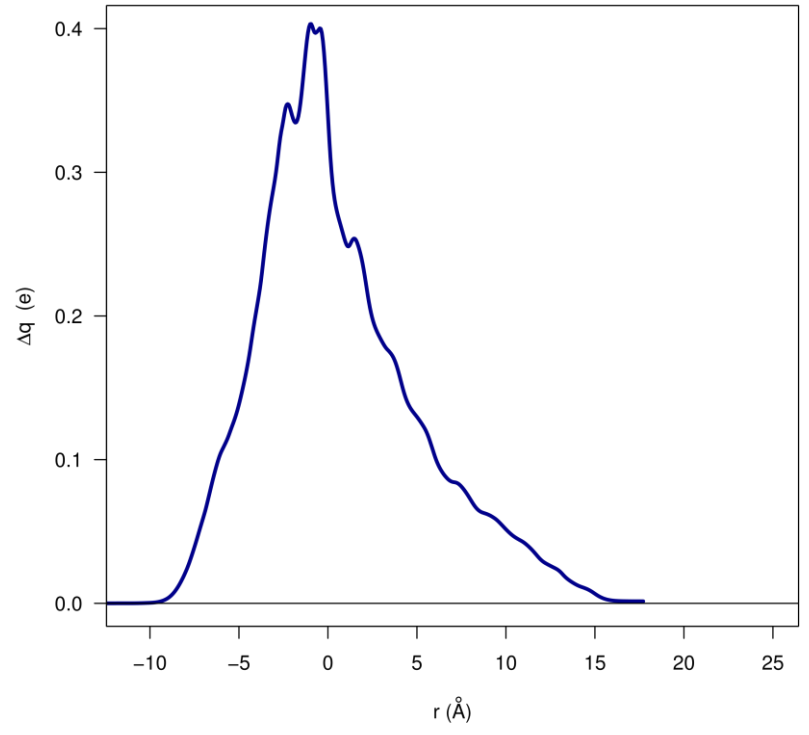

Fig. S3 : CD curve of the NKX-2587-TiO_2 system. The sensitizer is anchored on TiO_2 in BB geometry.

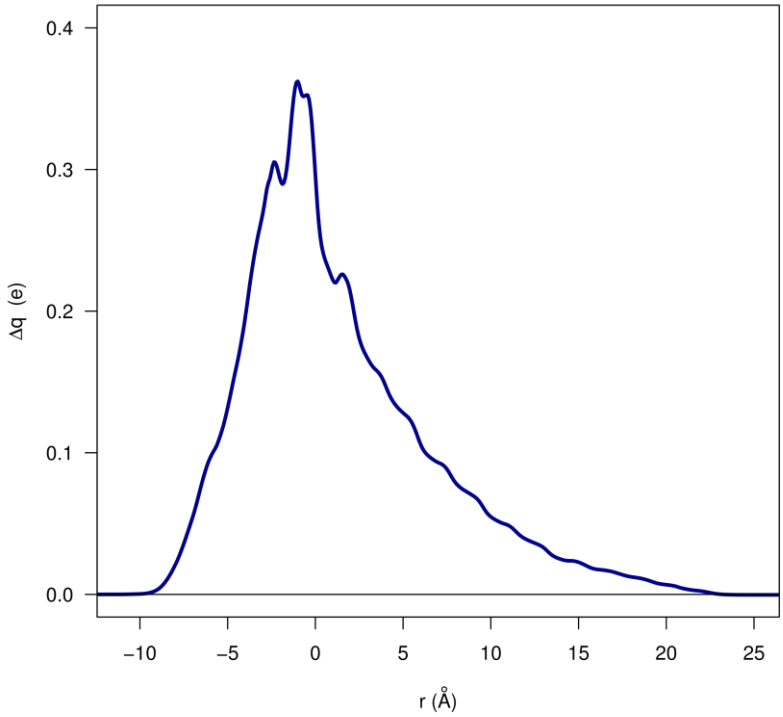

Fig. S4: CD curve of the NKX-2697-TiO_2 system. The sensitizer is anchored on TiO_2 in BB geometry.

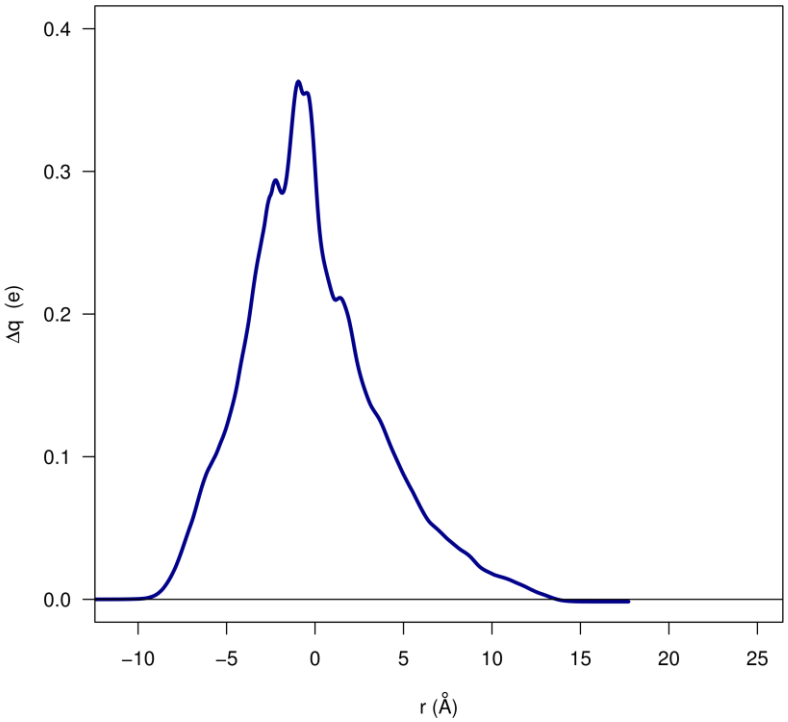

Fig. S5: CD curve of the L1-TiO_2 system. The sensitizer is anchored on TiO_2 in BB geometry.

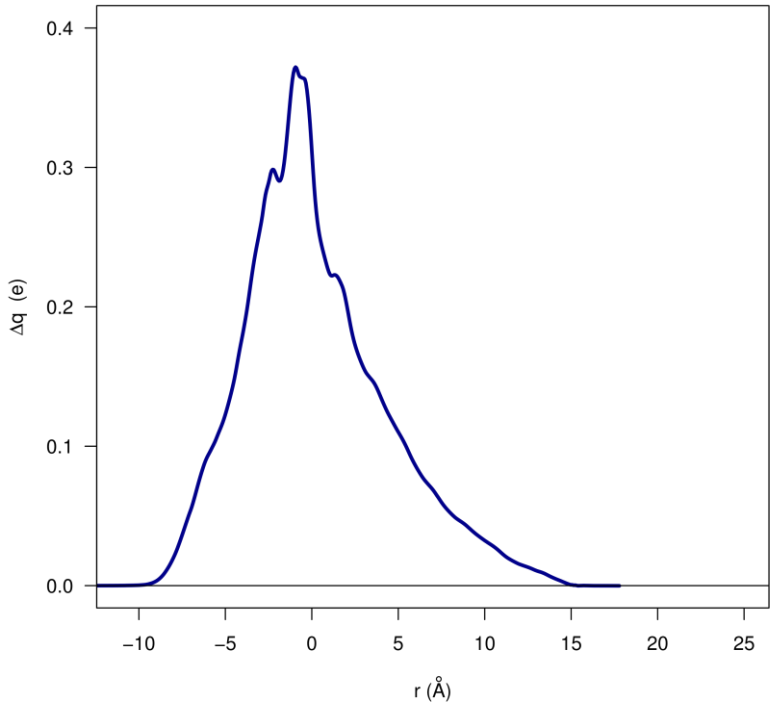

Fig. S6 : CD curve of the D5-TiO_2 system. The sensitizer is anchored on TiO_2 in BB geometry.

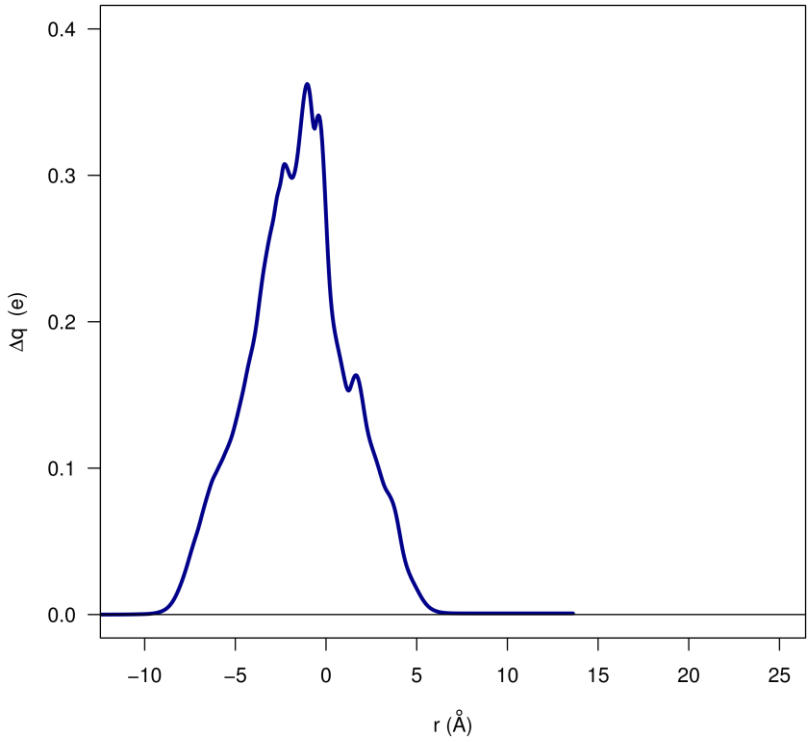

Fig. S7: CD curve of the BA-TiO_2 system. The sensitizer is anchored on TiO_2 in BB geometry.

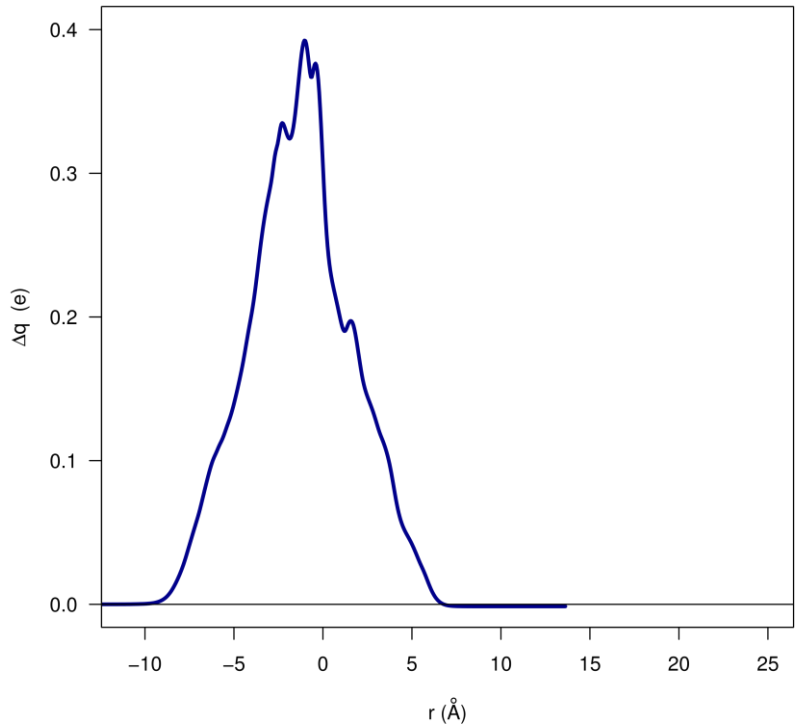

Fig. S8 : CD curve of the NH_2-BA-TiO_2 system. The sensitizer is anchored on TiO_2 in BB geometry.

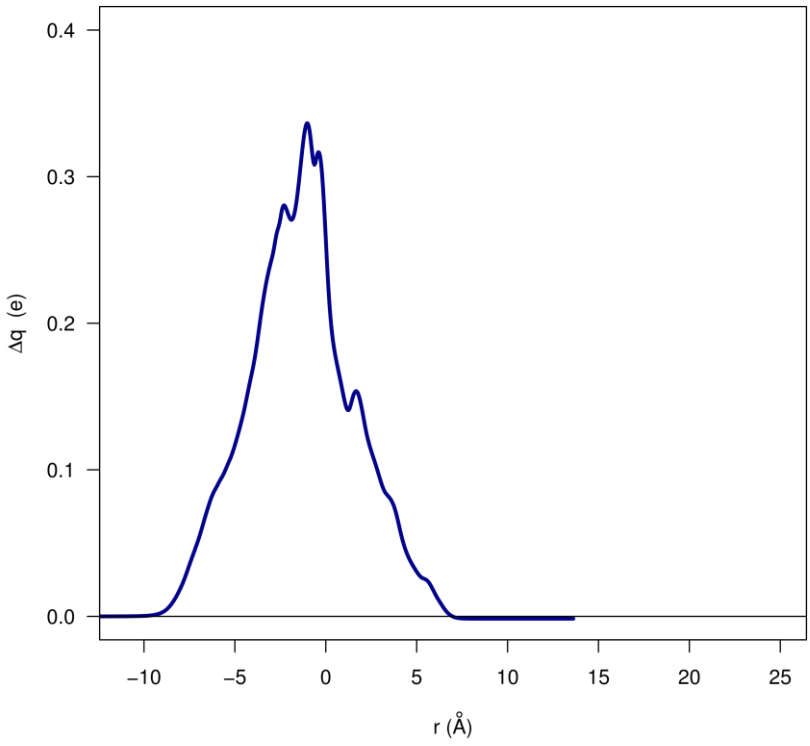

Fig. S9: CD curve of the NO_2-BA-TiO_2 system. The sensitizer is anchored on TiO_2 in BB geometry.

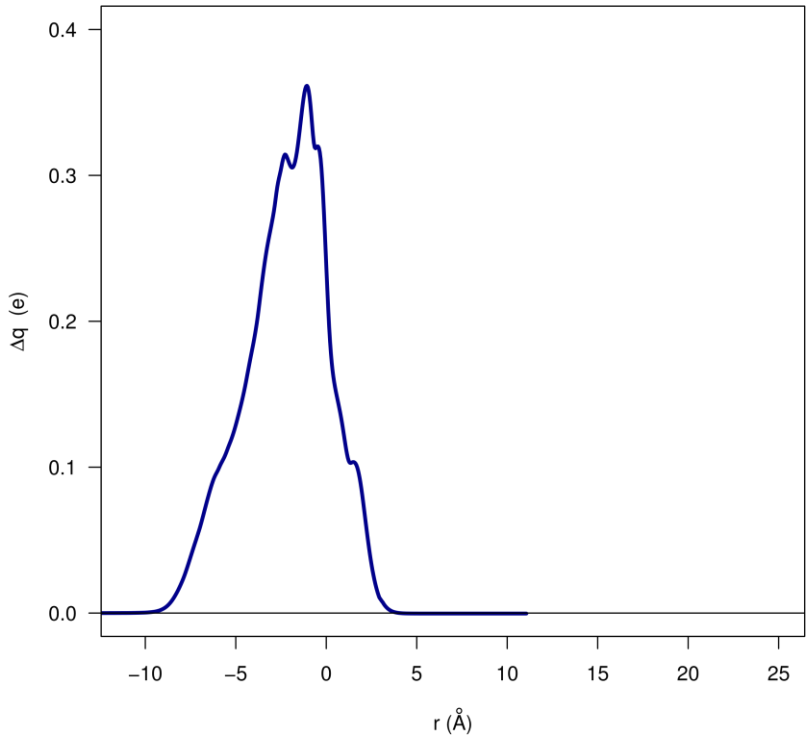

Fig. S10: CD curve of the AA-TiO_2 system. The sensitizer is anchored on TiO_2 in BB geometry.

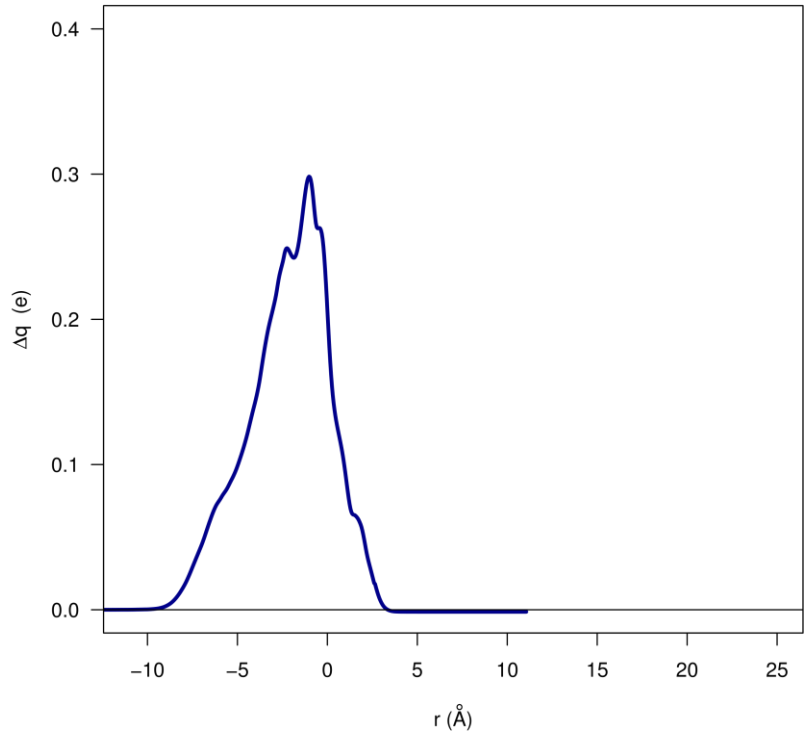

Fig S11: CD curve of the AAF_3-TiO_2 system. The sensitizer is anchored on TiO_2 in BB geometry.

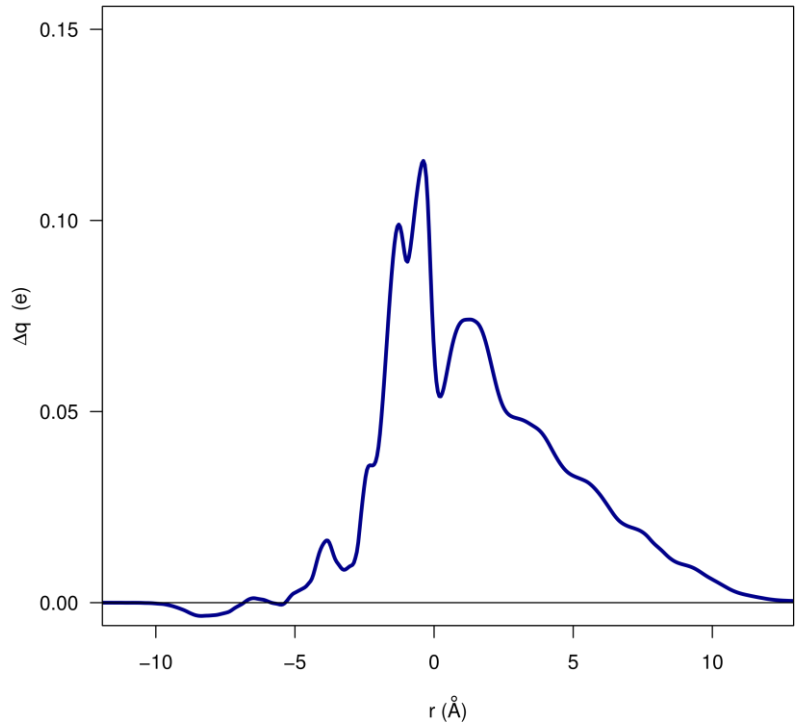

Fig. S12 : CD curve of the L0-TiO_2 system. The sensitizer is anchored on TiO_2 in M geometry.

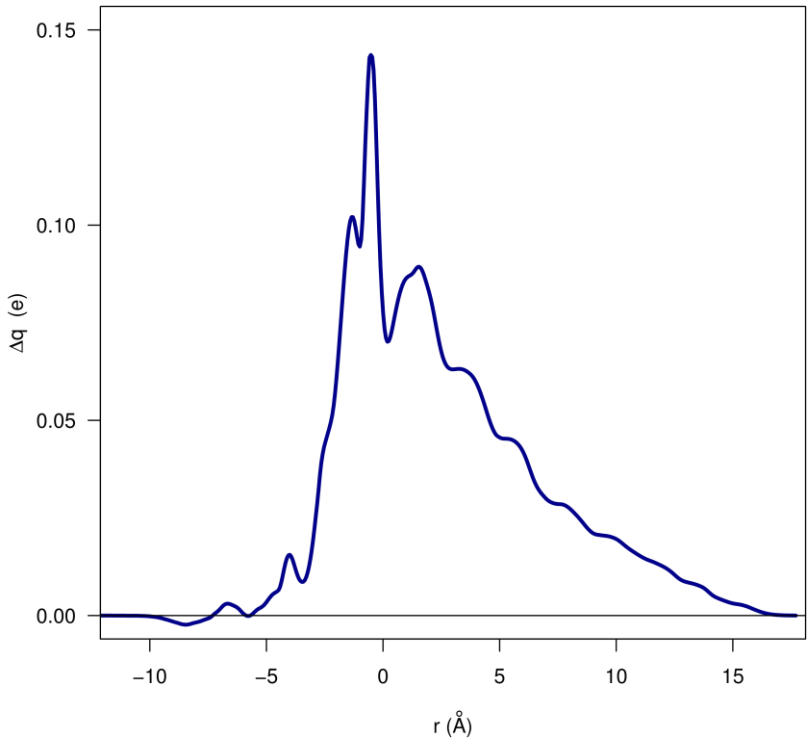

Fig. S13: CD curve of the NKX-2587-TiO_2 system. The sensitizer is anchored on TiO_2 in M geometry.

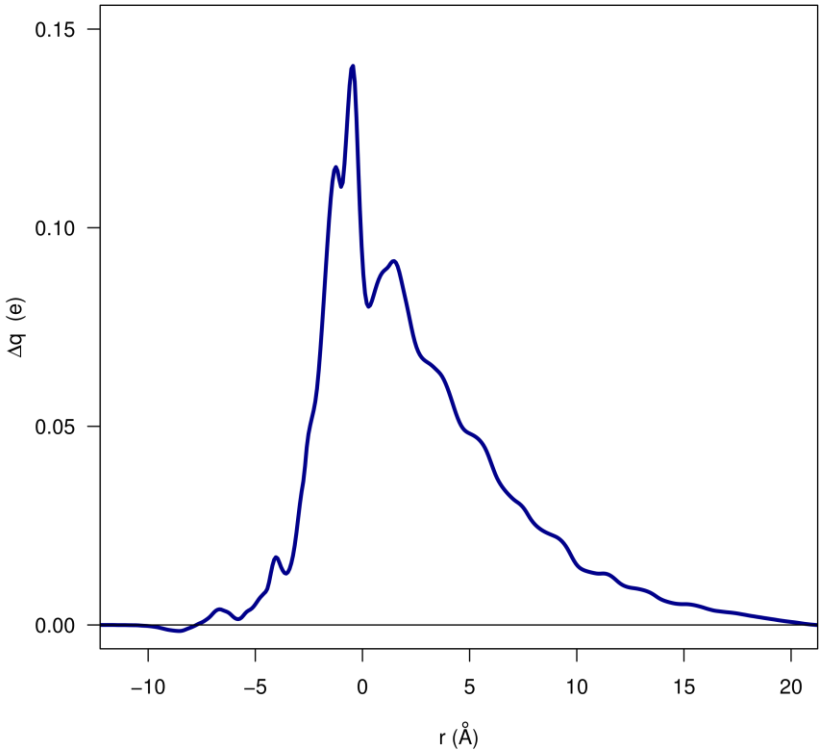

Fig. S14: CD curve of the NKX-2697-TiO_2 system. The sensitizer is anchored on TiO_2 in M geometry.

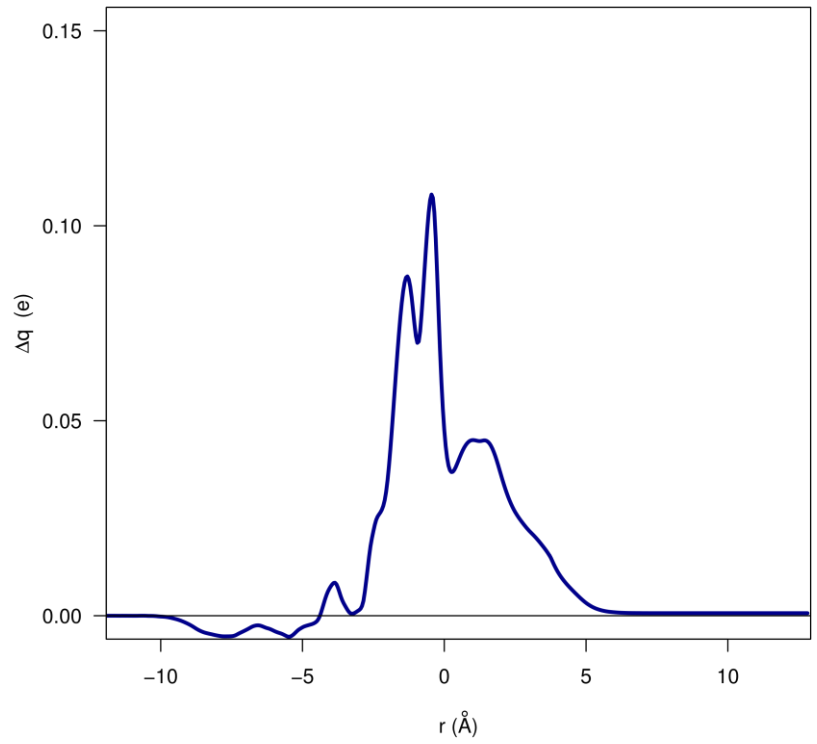

Fig. S15: CD curve of the BA-TiO_2 system. The sensitizer is anchored on TiO_2 in M geometry.

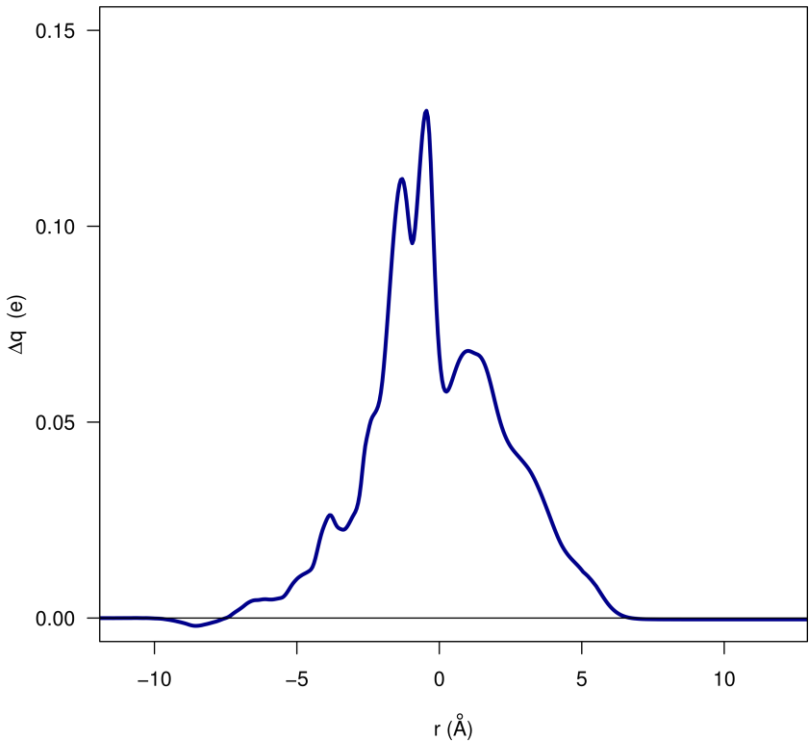

Fig. S16: CD curve of the NH_2-BA-TiO_2 system. The sensitizer is anchored on TiO_2 in M geometry.

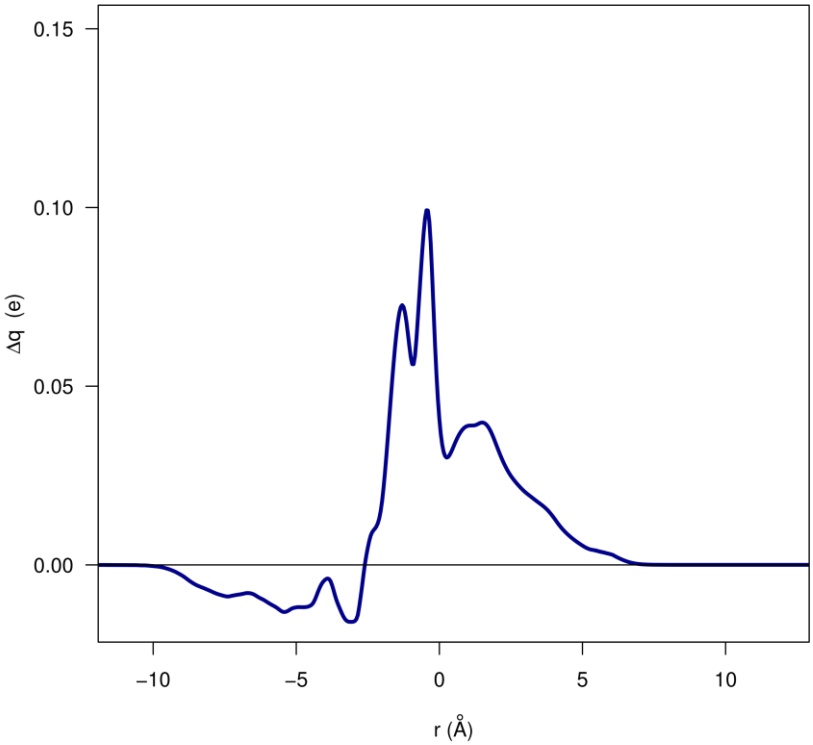

Fig. S17: CD curve of the NO_2-BA-TiO_2 system. The sensitizer is anchored on TiO_2 in M geometry.

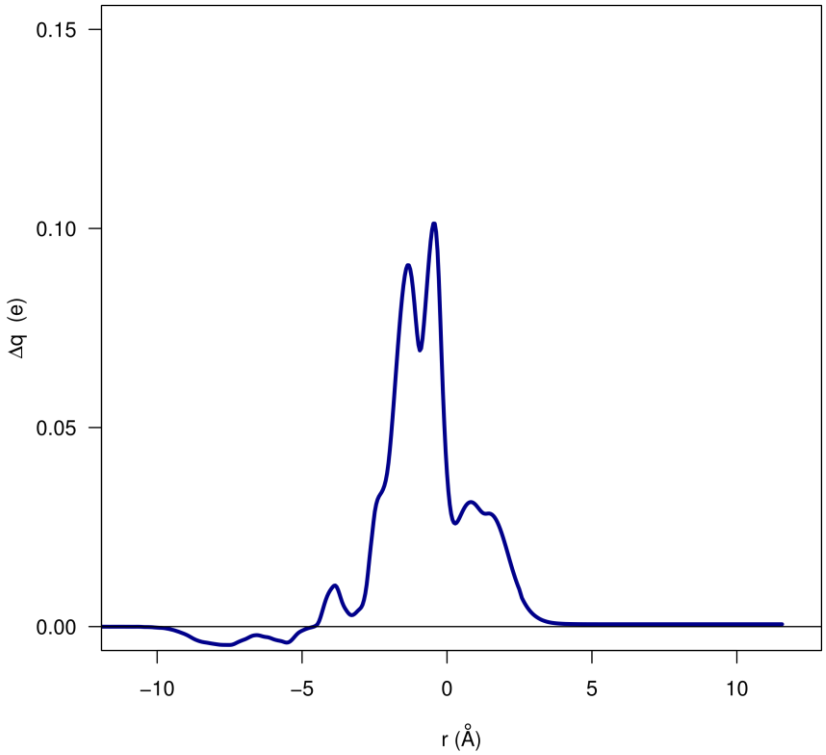

Fig. S18: CD curve of the AA-TiO_2 system. The sensitizer is anchored on TiO_2 in M geometry.

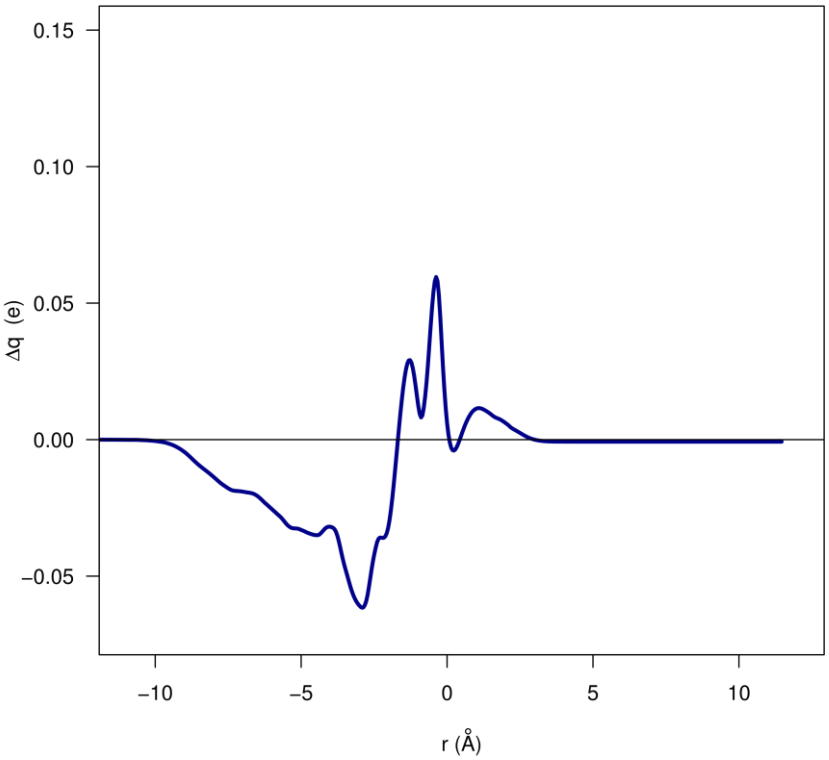

Fig. S19: CD curve of the AAF_3-TiO_2 system. The sensitizer is anchored on TiO_2 in M geometry.

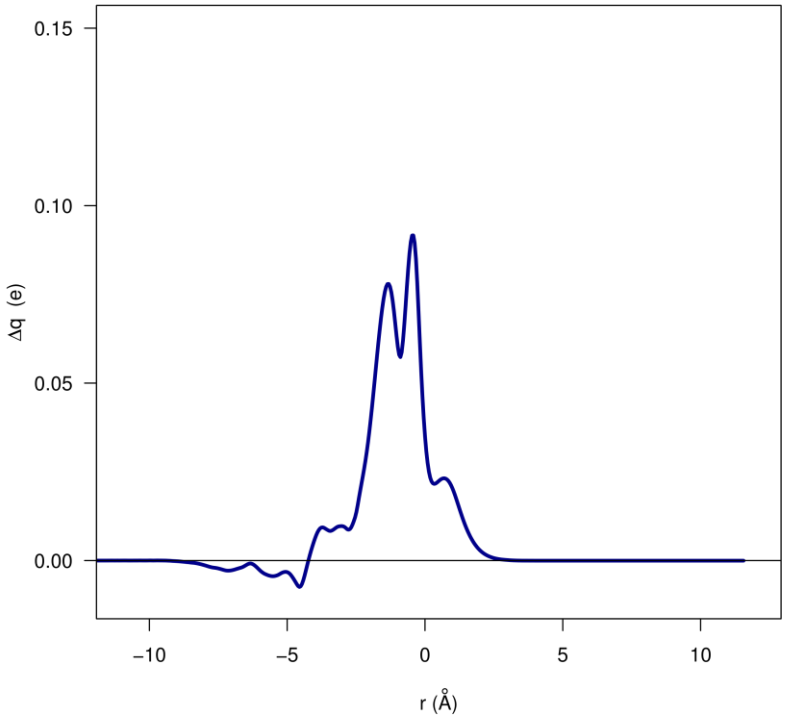

Fig. S20: CD curve of the FA-TiO_2 system. The sensitizer is anchored on TiO_2 in M geometry.

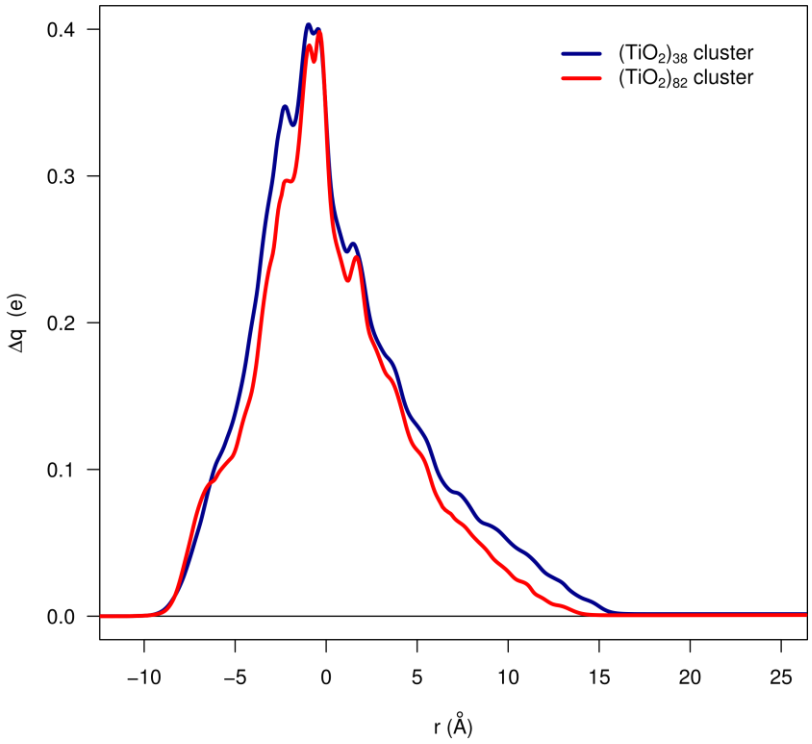

Fig. S21: Comparison between CD curves of the NKX-2587 dye anchored on a $(TiO_2)_{38}$ and $(TiO_2)_{82}$ clusters. The sensitizer is anchored on TiO_2 in BB geometry.

Partial Density of States (PDOS)

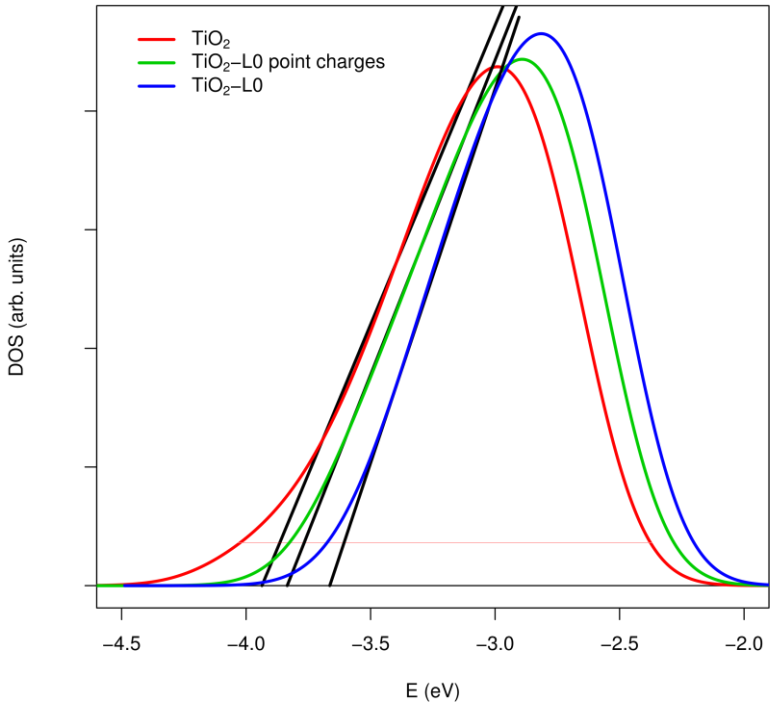

Fig. S22 : Plots of Density Of States (DOS) for the complex containing the L0 dye in the BB anchoring geometry: (red) $(TiO_2)_{38}$ cluster DOS, (green) DOS of the $(TiO_2)_{38}$ cluster in the presence of the point charges reproducing the dye electrostatic potential, (blue) $(TiO_2)_{38}$ cluster contribution to the total DOS.

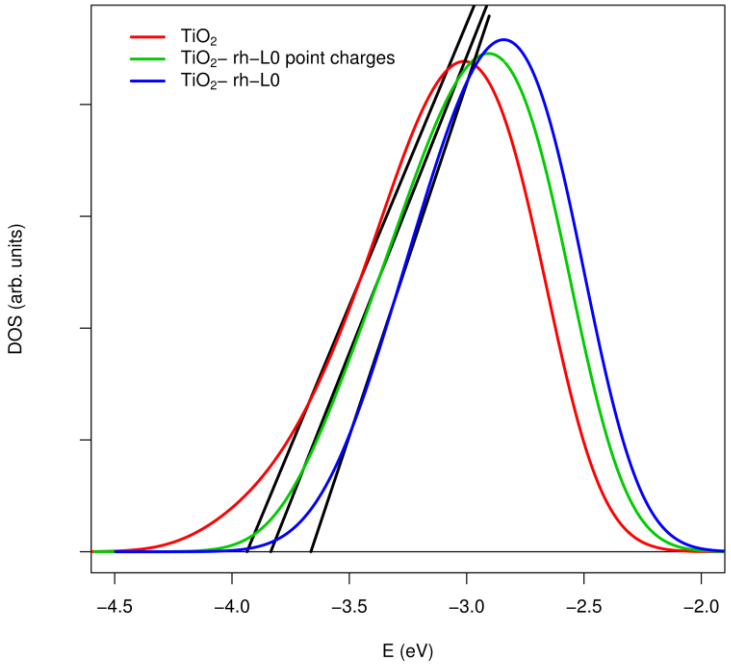

Fig. S23 : Plots of Density Of States (DOS) for the complex containing the rh-L0 dye in the BB anchoring geometry: (red) $(TiO_2)_{38}$ cluster DOS, (green) DOS of the $(TiO_2)_{38}$ cluster in the presence of the point charges reproducing the dye electrostatic potential, (blue) $(TiO_2)_{38}$ cluster contribution to the total DOS.

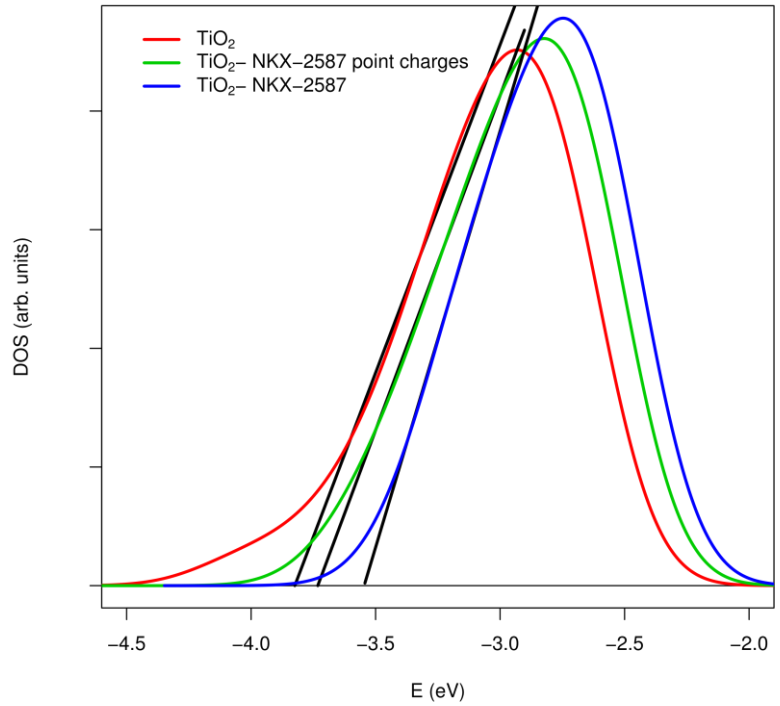

Fig. S24 : Plots of Density Of States (DOS) for the complex containing the NKX-2587 dye in the BB anchoring geometry: (red) $(TiO_2)_{38}$ cluster DOS, (green) DOS of the $(TiO_2)_{38}$ cluster in the presence of the point charges reproducing the dye electrostatic potential, (blue) $(TiO_2)_{38}$ cluster contribution to the total DOS.

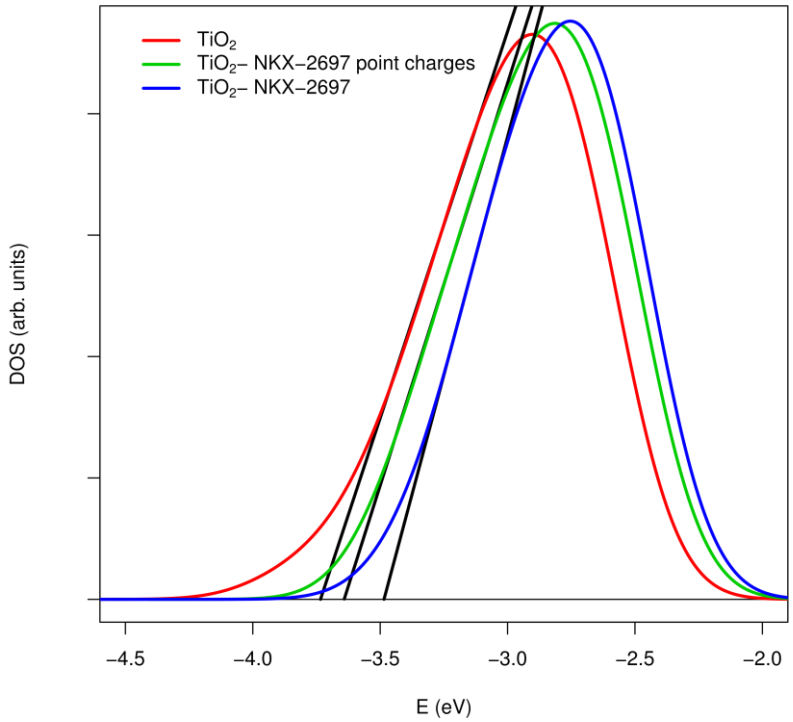

Fig. S25 : Plots of Density Of States (DOS) for the complex containing the NKX-2697 dye in the BB anchoring geometry: (red) $(TiO_2)_{38}$ cluster DOS, (green) DOS of the $(TiO_2)_{38}$ cluster in the presence of the point charges reproducing the dye electrostatic potential, (blue) $(TiO_2)_{38}$ cluster contribution to the total DOS.

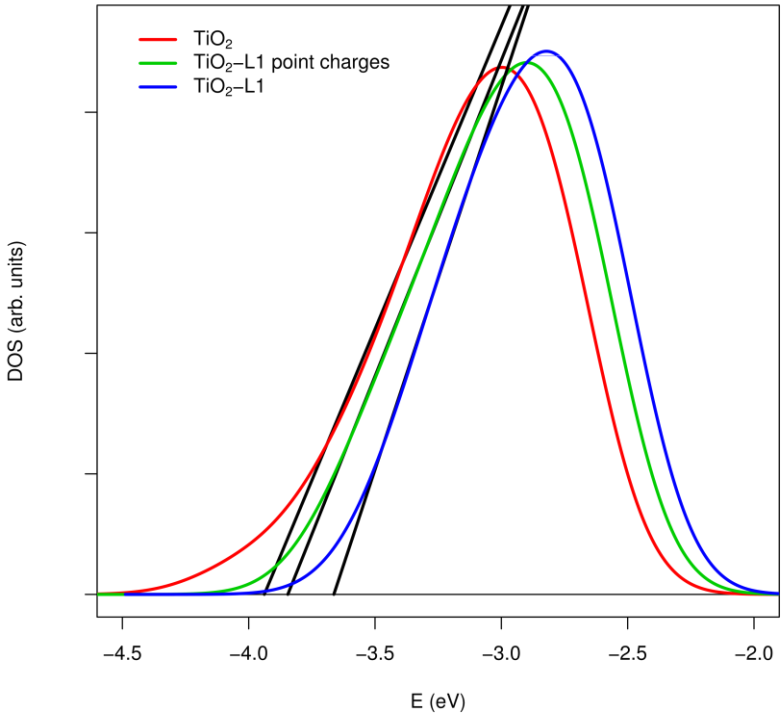

Fig. S26 : Plots of Density Of States (DOS) for the complex containing the L1 dye in the BB anchoring geometry: (red) $(TiO_2)_{38}$ cluster DOS, (green) DOS of the $(TiO_2)_{38}$ cluster in the presence of the point charges reproducing the dye electrostatic potential, (blue) $(TiO_2)_{38}$ cluster contribution to the total DOS.

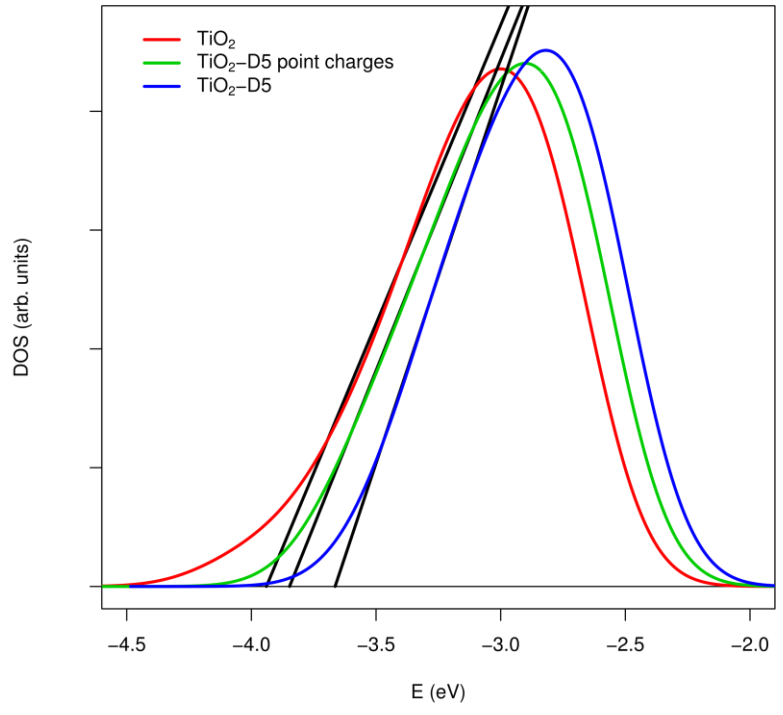

Fig. S27 : Plots of Density Of States (DOS) for the complex containing the D5 dye in the BB anchoring geometry: (red) $(TiO_2)_{38}$ cluster DOS, (green) DOS of the $(TiO_2)_{38}$ cluster in the presence of the point charges reproducing the dye electrostatic potential, (blue) $(TiO_2)_{38}$ cluster contribution to the total DOS.

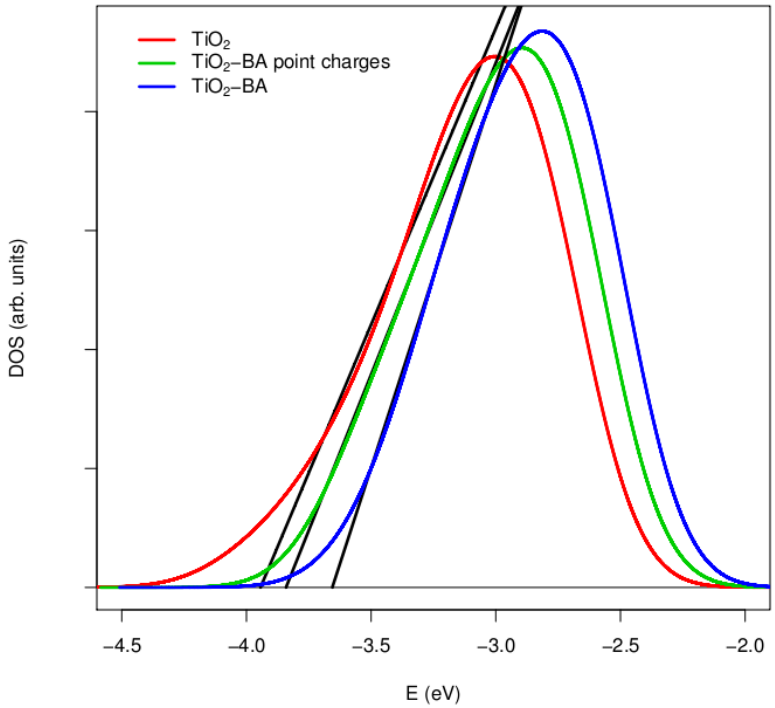

Fig. S28 : Plots of Density Of States (DOS) for the complex containing BA in the BB anchoring geometry: (red) $(TiO_2)_{38}$ cluster DOS, (green) DOS of the $(TiO_2)_{38}$ cluster in the presence of the point charges reproducing the dye electrostatic potential, (blue) $(TiO_2)_{38}$ cluster contribution to the total DOS.

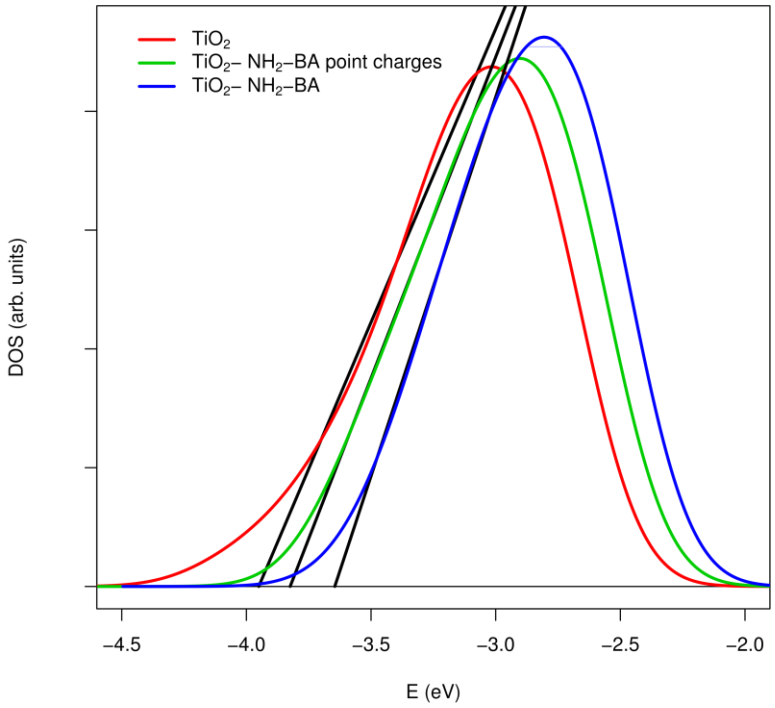

Fig. S29 : Plots of Density Of States (DOS) for the complex containing NH_2-BA in the BB anchoring geometry: (red) $(TiO_2)_{38}$ cluster DOS, (green) DOS of the $(TiO_2)_{38}$ cluster in the presence of the point charges reproducing the dye electrostatic potential, (blue) $(TiO_2)_{38}$ cluster contribution to the total DOS.

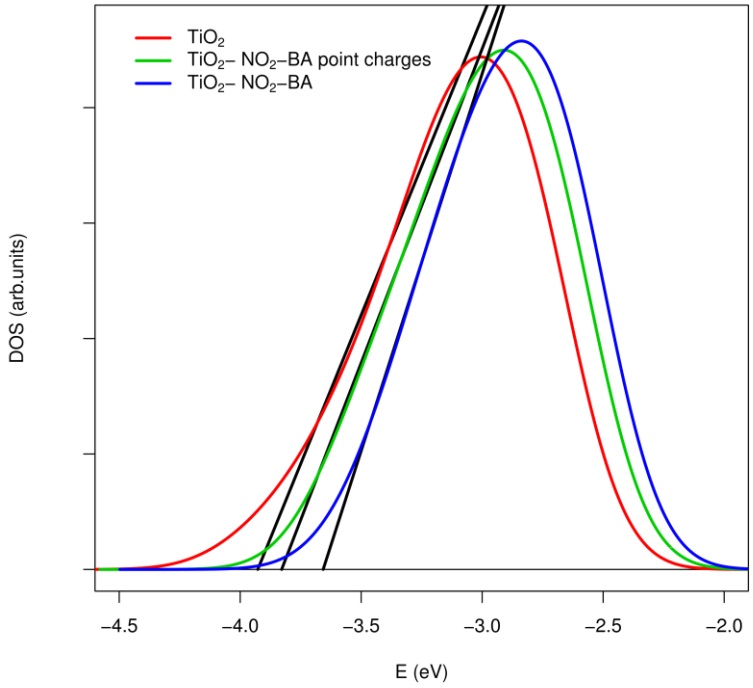

Fig. S30 : Plots of Density Of States (DOS) for the complex containing NO_2-BA in the BB anchoring geometry: (red) $(TiO_2)_{38}$ cluster DOS, (green) DOS of the $(TiO_2)_{38}$ cluster in the presence of the point charges reproducing the dye electrostatic potential, (blue) $(TiO_2)_{38}$ cluster contribution to the total DOS.

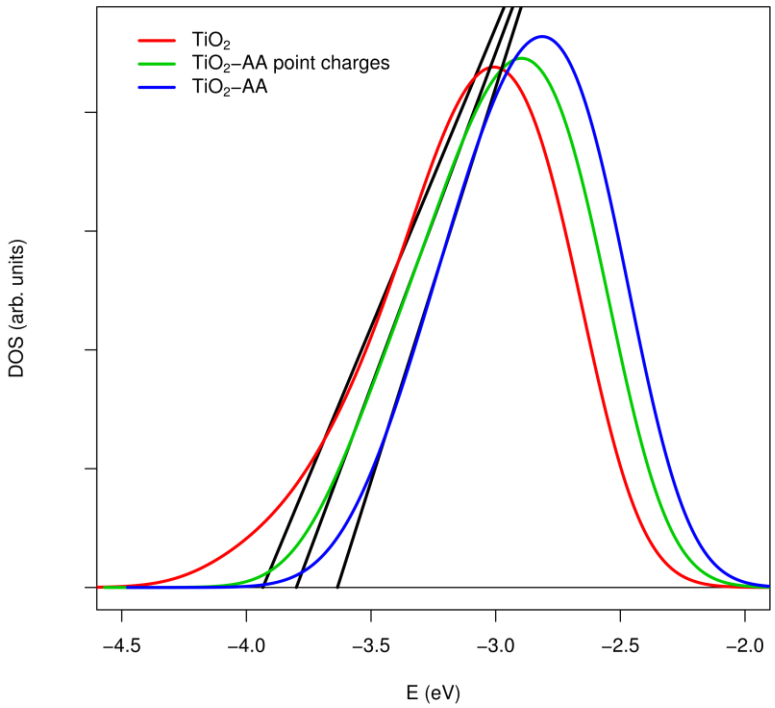

Fig. S31: Plots of Density Of States (DOS) for the complex containing AA in the BB anchoring geometry: (red) $(TiO_2)_{38}$ cluster DOS, (green) DOS of the $(TiO_2)_{38}$ cluster in the presence of the point charges reproducing the dye electrostatic potential, (blue) $(TiO_2)_{38}$ cluster contribution to the total DOS.

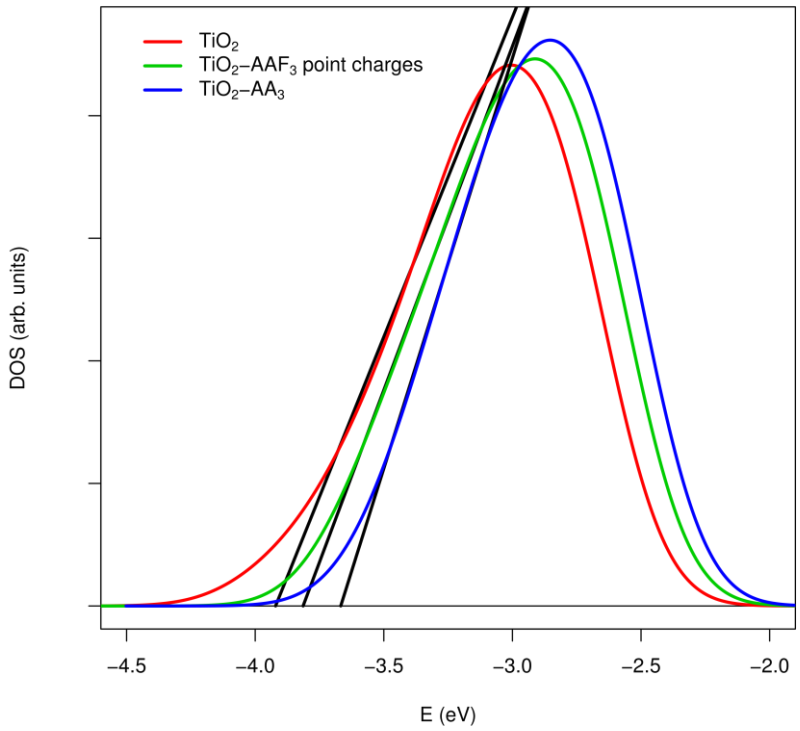

Fig. S32: Plots of Density Of States (DOS) for the complex containing AAF_3 in the BB anchoring geometry: (red) $(TiO_2)_{38}$ cluster DOS, (green) DOS of the $(TiO_2)_{38}$ cluster in the presence of the point charges reproducing the dye electrostatic potential, (blue) $(TiO_2)_{38}$ cluster contribution to the total DOS.

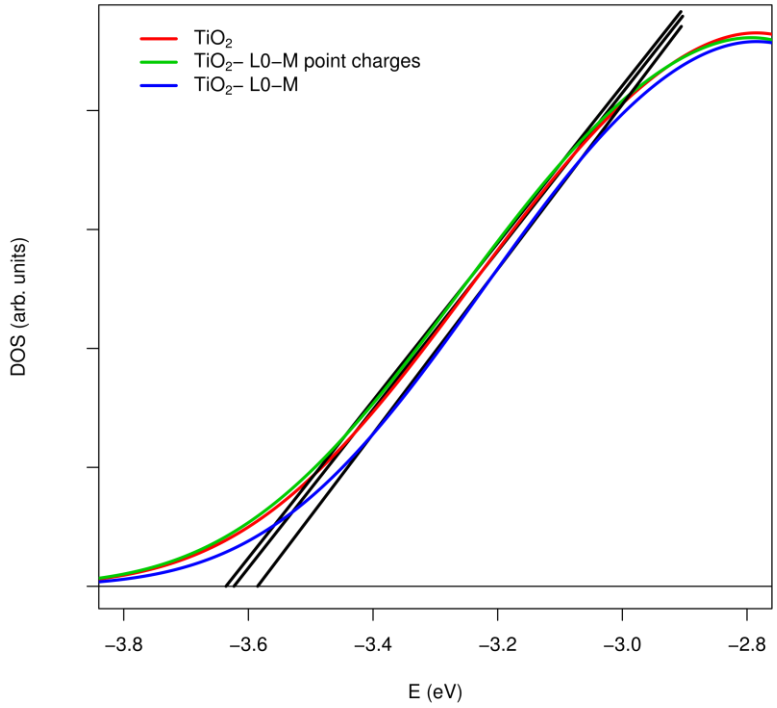

Fig. S33 : Plots of Density Of States (DOS) for the complex containing the L0 dye in the M anchoring geometry: (red) $(TiO_2)_{38}$ cluster DOS, (green) DOS of the $(TiO_2)_{38}$ cluster in the presence of the point charges reproducing the dye electrostatic potential, (blue) $(TiO_2)_{38}$ cluster contribution to the total DOS.

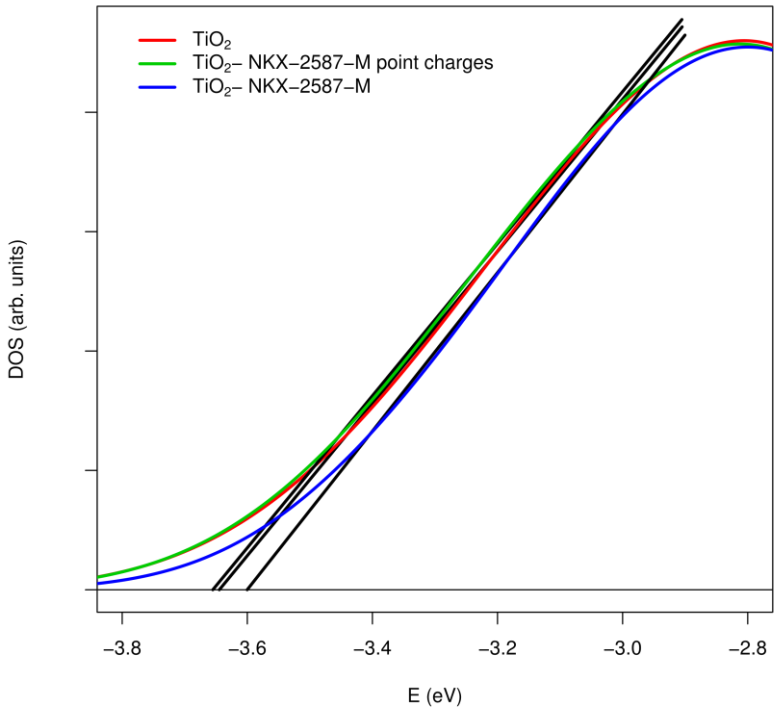

Fig. S34: Plots of Density Of States (DOS) for the complex containing the NKX-2587 dye in the M anchoring geometry: (red) $(TiO_2)_{38}$ cluster DOS, (green) DOS of the $(TiO_2)_{38}$ cluster in the presence of the point charges reproducing the dye electrostatic potential, (blue) $(TiO_2)_{38}$ cluster contribution to the total DOS.

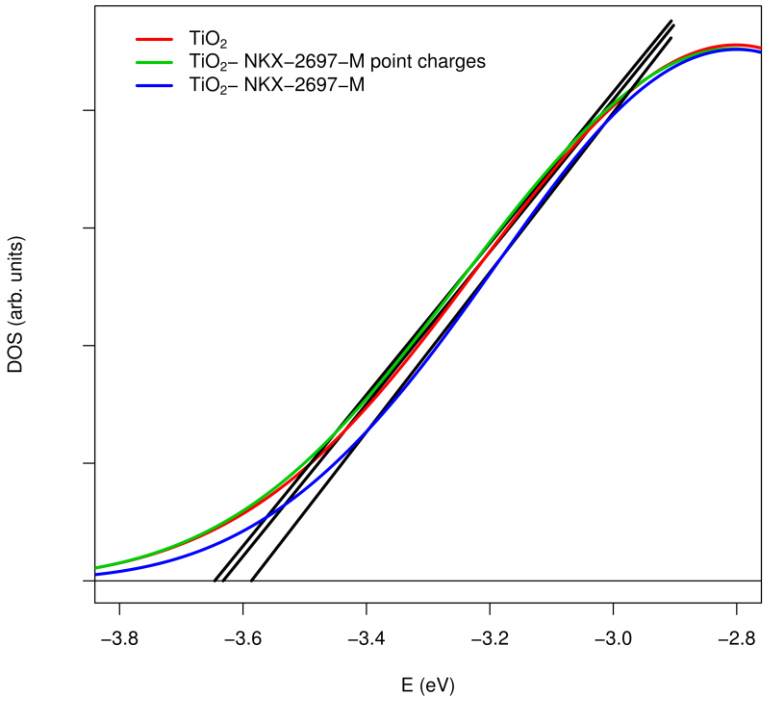

Fig. S35: Plots of Density Of States (DOS) for the complex containing the NKX-2697 dye in the M anchoring geometry: (red) $(TiO_2)_{38}$ cluster DOS, (green) DOS of the $(TiO_2)_{38}$ cluster in the presence of the point charges reproducing the dye electrostatic potential, (blue) $(TiO_2)_{38}$ cluster contribution to the total DOS.

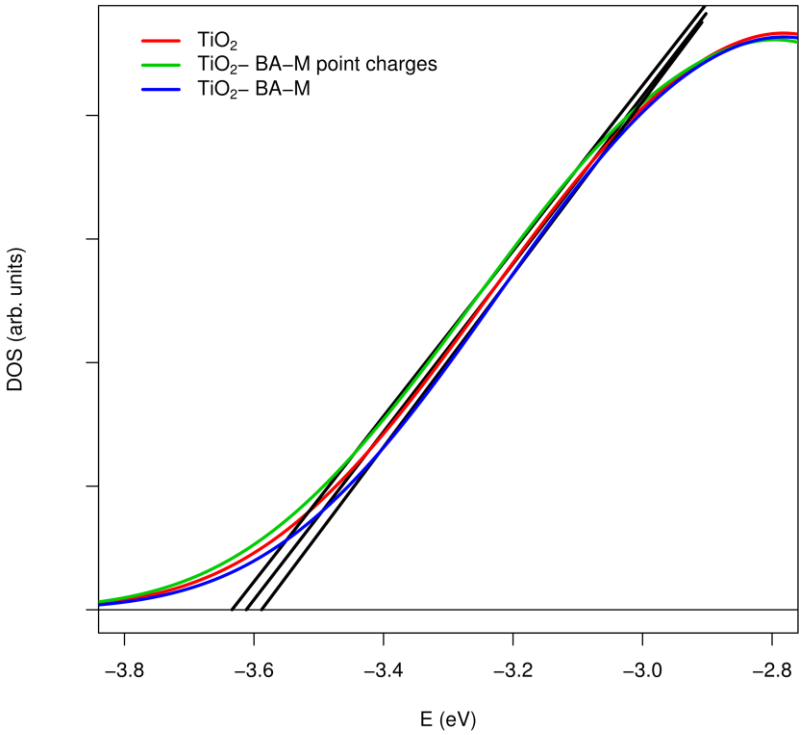

Fig. S36: Plots of Density Of States (DOS) for the complex containing the BA dye in the M anchoring geometry: (red) $(TiO_2)_{38}$ cluster DOS, (green) DOS of the $(TiO_2)_{38}$ cluster in the presence of the point charges reproducing the dye electrostatic potential, (blue) $(TiO_2)_{38}$ cluster contribution to the total DOS.

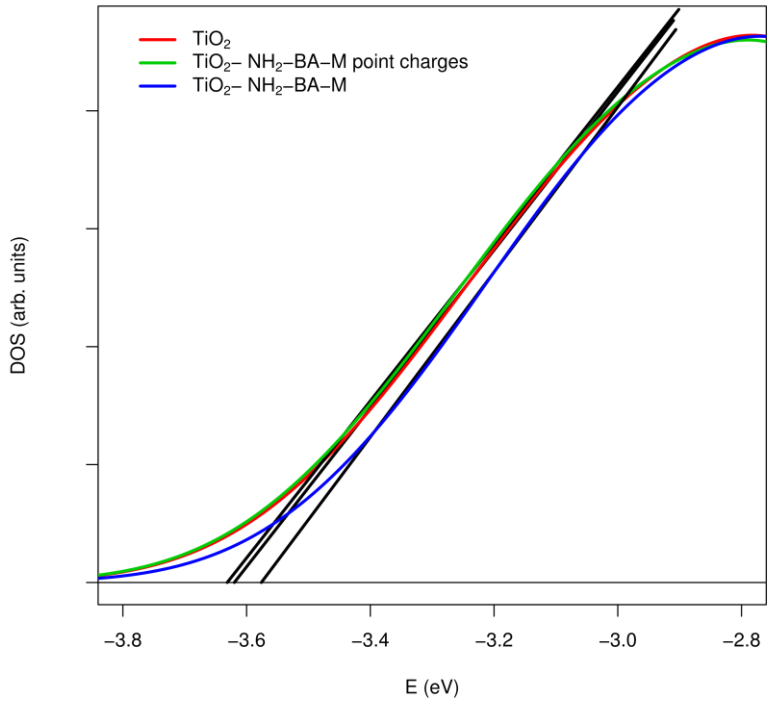

Fig. S37: Plots of Density Of States (DOS) for the complex containing the NH_2-BA dye in the M anchoring geometry: (red) $(TiO_2)_{38}$ cluster DOS, (green) DOS of the $(TiO_2)_{38}$ cluster in the presence of the point charges reproducing the dye electrostatic potential, (blue) $(TiO_2)_{38}$ cluster contribution to the total DOS.

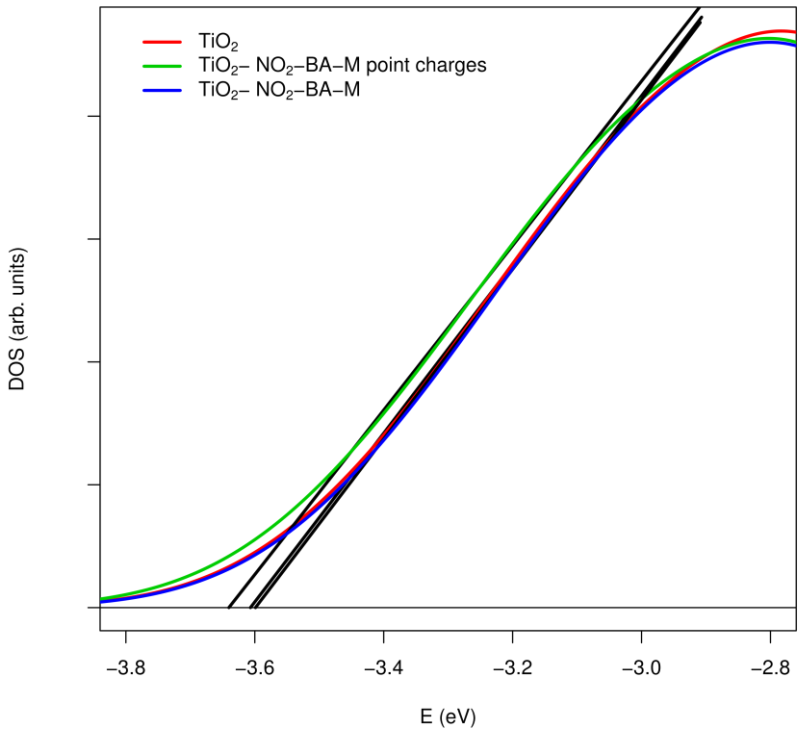

Fig. S38: Plots of Density Of States (DOS) for the complex containing the NO_2-BA dye in the M anchoring geometry: (red) $(TiO_2)_{38}$ cluster DOS, (green) DOS of the $(TiO_2)_{38}$ cluster in the presence of the point charges reproducing the dye electrostatic potential, (blue) $(TiO_2)_{38}$ cluster contribution to the total DOS.

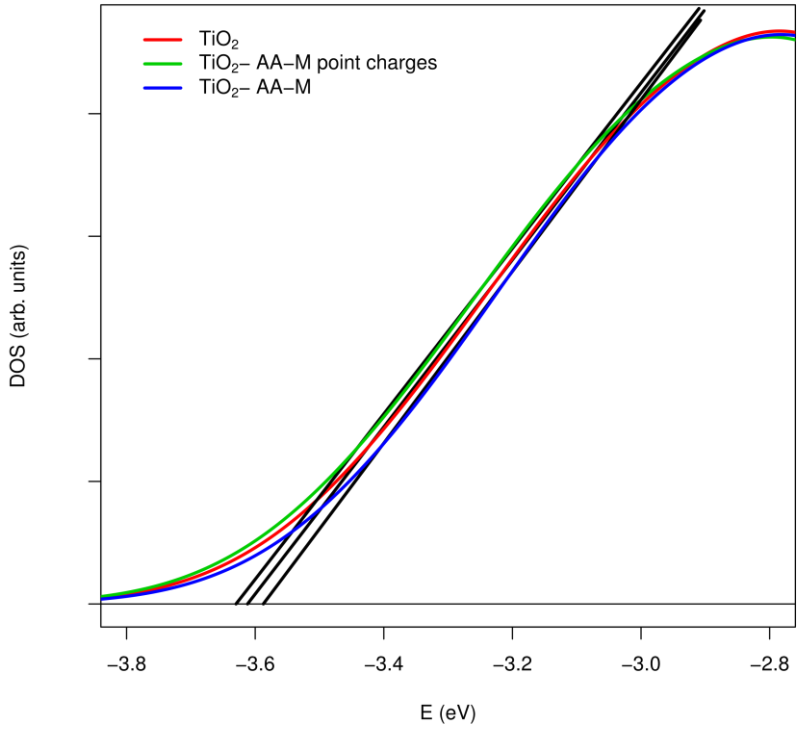

Fig. S39: Plots of Density Of States (DOS) for the complex containing the AA dye in the M anchoring geometry: (red) $(TiO_2)_{38}$ cluster DOS, (green) DOS of the $(TiO_2)_{38}$ cluster in the presence of the point charges reproducing the dye electrostatic potential, (blue) $(TiO_2)_{38}$ cluster contribution to the total DOS.

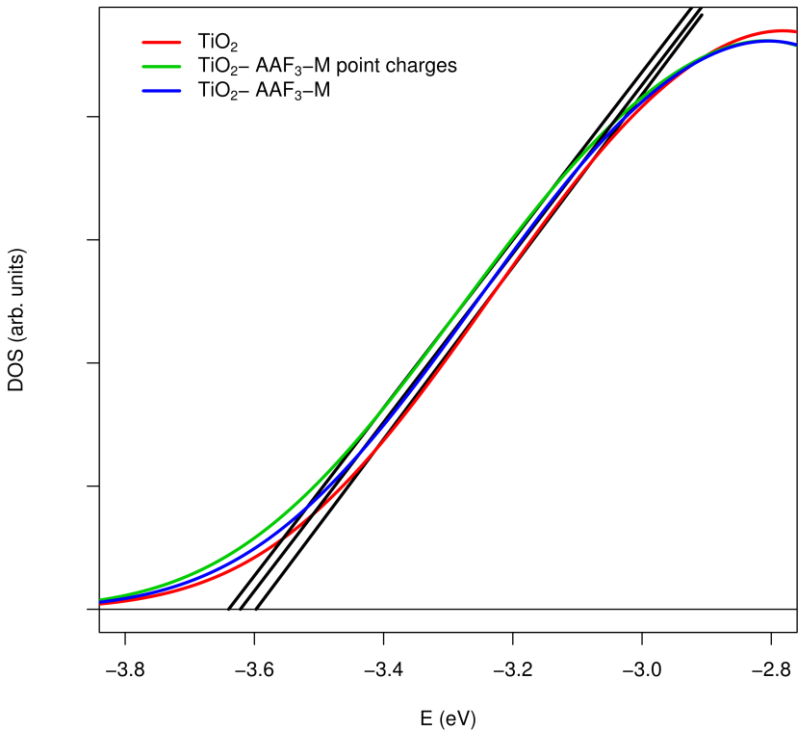

Fig. S40: Plots of Density Of States (DOS) for the complex containing the AAF_3 dye in the M anchoring geometry: (red) $(TiO_2)_{38}$ cluster DOS, (green) DOS of the $(TiO_2)_{38}$ cluster in the presence of the point charges reproducing the dye electrostatic potential, (blue) $(TiO_2)_{38}$ cluster contribution to the total DOS.

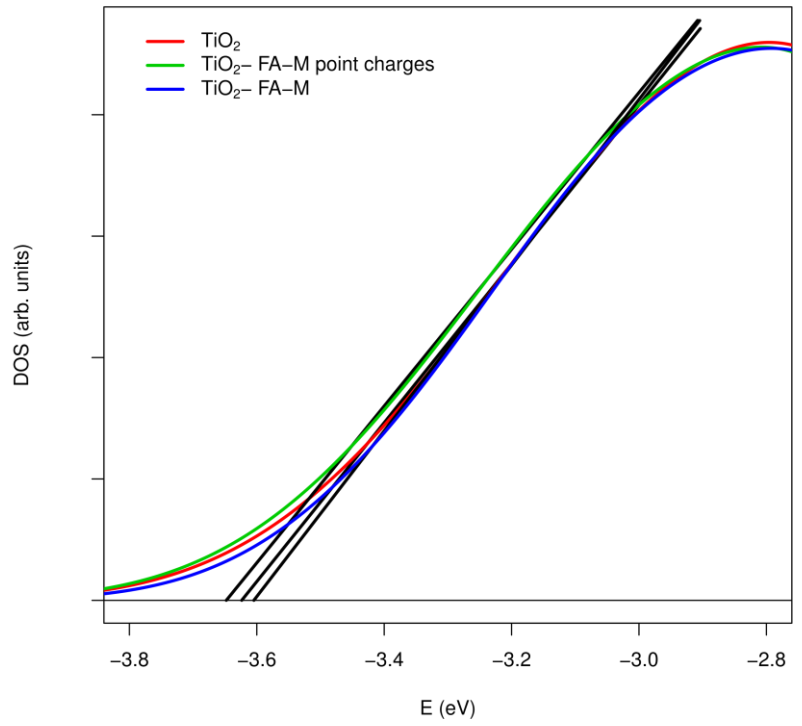

Fig. S41: Plots of Density Of States (DOS) for the complex containing the FA dye in the M anchoring geometry: (red) $(TiO_2)_{38}$ cluster DOS, (green) DOS of the $(TiO_2)_{38}$ cluster in the presence of the point charges reproducing the dye electrostatic potential, (blue) $(TiO_2)_{38}$ cluster contribution to the total DOS.

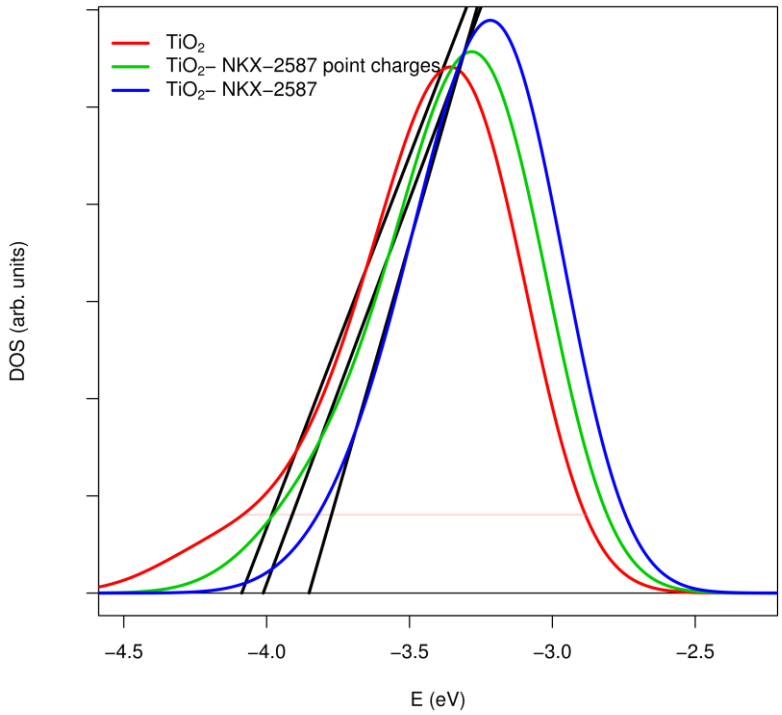

Fig. S42 : Plots of Density Of States (DOS) for the complex containing the NKX-2587 dye in the BB anchoring geometry: (red) $(TiO_2)_{82}$ cluster DOS, (green) DOS of the $(TiO_2)_{82}$ cluster in the presence of the point charges reproducing the dye electrostatic potential, (blue) $(TiO_2)_{82}$ cluster contribution to the total DOS.

Table S1. Comparison between the amount of CT calculated from the CD curves and from the partial dye charges for the interacting dye/semiconductor assemblies.

System	Charges CT	CD CT
L0-BB	**0.43**	**0.36**
NKX-2587-BB	**0.39**	**0.40**
NKX-2697-BB	**0.34**	**0.36**
L1-BB	**0.40**	**0.36**
AA-BB	**0.48**	**0.36**

Additional fit

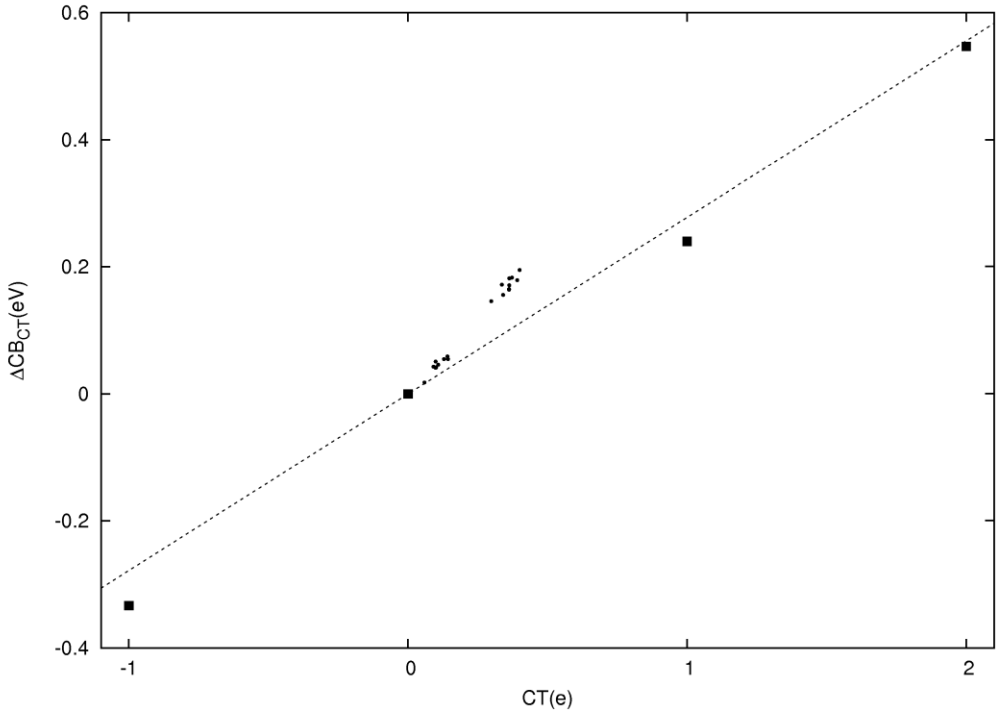

Fig. S43: Effect of charge donation/withdrawal on the energy position of the conduction band edge. When two electron are added to TiO_2 we calculated the shifts relative to both singlet and triplet electronic state, finding almost coincident values.